Synthesis, photopolymerization kinetics, and thermal properties of UV-curable waterborne hyperbranched polyurethane acrylate dispersions

Wenhua Yin, Xingrong Zeng, Hongqiang Li, Youjun Hou, Qiongzhi Gao

Abstract A series of UV-curable waterborne hyperbranched polyurethane acrylate dispersions (WHBPUADs) were prepared via a three-step procedure based on isophorone diisocyanate (IPDI), hyperbranched polyester (HBP), maleic anhydride (MA), and hydroxy-ethyl acrylate (HEA). The structure of WHBPUADs was characterized by Fourier transform infrared spectroscopy (FTIR) and ^{1}H nuclear magnetic resonance spectroscopy (^{1}H NMR). FTIR was also applied to research the effect of double bond concentration on the kinetics of photopolymerization. The heat resistance of the cured films was characterized by thermogravimetric analysis (TGA), and their mechanical properties were also measured. The results showed that the double bond conversion (τ) and photopolymerization rate (R_p) were affected by the concentration of double bond and viscosity of WHBPUADs. The UV-curable systems with higher double bond concentration and lower viscosity led to higher τ and R_p. The maximum τ and R_p reached 93% and 71 mmol g^{-1} s^{-1}, respectively. The WHBPUADs films possessed better heat resistance and mechanical properties, and with the increase of crosslink density, the heat resistance and hardnesses were further improved.

Keywords UV-curable, Waterborne, Hyperbranched polyurethane acrylate, FTIR, Photopolymerization kinetics

W. Yin, X. Zeng (✉), H. Li, Y. Hou, Q. Gao
College of Materials Science and Engineering, South China University of Technology, Guangzhou 510640, China
e-mail: psxrzeng@gmail.com

Q. Gao
College of Science, South China Agricultural University, Guangzhou 510640, China

Introduction

With ever-increasing environmental awareness, more and more countries have issued a series of related laws and regulations to limit the emissions of volatile organic compound (VOC). Therefore, research on the development of new coating systems such as waterborne, radiation curable, and powder coatings has increased dramatically in recent years.

Waterborne UV-curable technology, which combines the environmental friendliness and the versatility of waterborne polymers with the rapid curing and low energy consumption of UV-curable systems, has generated wide interest due to its extensive application in coatings and adhesives for various substrates.[1,2] Acrylic, epoxy, and polyurethane acrylate are the three typical UV-curable matrix resins. Among the resins, polyurethane acrylate has been most widely applied because of its comprehensive properties, such as superior resistance to abrasion and scratch, and high impact and tensile strength of the cured polymer, especially when hyperbranched groups have been introduced into the backbone of polyurethane acrylate polymer.[3–5] Whether in industrial production or academic research, the photopolymerization kinetics are worth studying along with the mechanical properties of the UV-curable system. However, there are few pioneering investigations of the photopolymerization kinetics of UV-curable waterborne hyperbranched polyurethane acrylate system. Photo-DSC has been extensively applied to monitor the UV-curing reactions.[6,7] However, it is impossible to follow reactions which occur in <1 min due to the rather long response time of a calorimeter device and a low thermal conductivity of most of the samples under the common irradiation conditions.[8,9] Fourier transform infrared spectroscopy (FTIR) has a wide range of applications in structural identification and the monitoring of reactions without such

limitations. In comparison to photo-DSC, this technique is convenient and can provide sufficient time resolution and relatively more accurate results in a quantitative determination.[10,11]

In our previous studies, a type of UV-curable solventborne hyperbranched polyurethane acrylate coatings system was prepared, and the UV-curing behavior, the mechanical properties and the heat resistance of the UV-cured films had been discussed.[12,13] This article describes the preparation and properties of the UV-curable waterborne hyperbranched polyurethane acrylate dispersions (WHBPUADs). For this purpose, NCO terminal prepolymer (prepolymer I) and COOH terminal prepolymer (prepolymer II) were first produced by addition and monoesterification reaction, respectively. Then, the two prepolymers were mixed for further reaction to obtain WHBPUADs. FTIR was used to characterize the structure and study the kinetics of photopolymerization of WHBPUADs. The mechanical properties and the heat resistance of the cured films were also investigated.

Experimental

Materials

The hyperbranched polyester (HBP), Boltorn®H20, is an ideal second generation hyperbranched aliphatic polyester and was purchased from Perstorp Specialty Chemicals AB, Sweden, with a molecular weight of 1748 g mol^{-1} and theoretically 16 primary end hydroxyl groups. The ideal structure of HBP is shown in Fig. 1. Maleic anhydride (MA) was purchased from Tianjin No. 1 Chemical Reagent Factory, China.
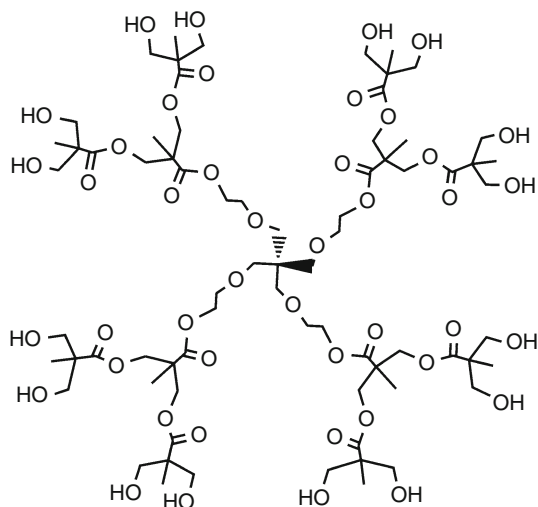

Fig. 1: Molecular architecture of HBP

Isophorone diisocyanate (IPDI) was supplied by Degussa-Huels Pacific Ltd., Germany and used without any further purification. 2-Hydroxyethyl acrylate (HEA), tetrahydrofuran (THF), and triethylamine (TEA) were purchased from Shanghai Chemical Co., China, and used after drying over 4 Å molecular sieves. 4-Dimethylaminopyridine (DMAP) and dibutyltin dilaurate (DBTDL) were purchased from GE Co., USA. 2-Hydroxyl-2-methyl-1-phenyl-1-propanone (Darocur 1173) acted as a photoinitiator and was supplied by Ciba, Switzerland.

Synthesis of WHBPUADs

Synthesis of prepolymer

The prepolymer was synthesized via a three-step procedure in a 250 mL four-necked, round-bottomed flask equipped with a mechanical stirrer, a thermometer, a dropping funnel, an inlet of dry nitrogen, and a reflux condenser with a drying tube. The reaction scheme is shown in Fig. 2. Taking WHBPUAD 8-8, for example, the process of synthesis is described in the following paragraphs.

In the first step, the prepolymer I was synthesized under a nitrogen atmosphere by reacting IPDI (10.18 g, 45.79 mmol) with HEA (5.32 g, 45.79 mmol) at 40°C with continuous stirring in the presence of DBTDL (ca. 0.05 g). The isocyanate (NCO) content in the prepolymer reached a constant value at about 4 h. The NCO content in the prepolymer was 12.4%, which was determined by the standard dibutylamine back titration method (ASTM D2572).

In the second step, to a solution of HBP (10.0 g, 5.72 mmol) in THF (50 mL) were added MA (4.49 g, 45.79 mmol) and a catalytic amount of DMAP (ca. 100 mg), and the mixture was stirred for 10 h at 50°C until the anhydride peak at 1784 cm^{-1} in the FTIR spectrum disappeared. The obtained resin (prepolymer II) was a transparent yellow liquid that theoretically has eight hydroxyl groups modified to –COOH groups.

In the third step, the WHBPUA was synthesized by adding dropwise prepolymer I into prepolymer II at 50°C for about 5 h until the peak at 2270 cm^{-1} for –NCO groups completely disappeared.

Neutralization and dispersion

The WHBPUA was cooled to 40°C, and the carboxylic groups were neutralized with TEA (4.63 g, 45.79 mmol) for 30 min. Finally, the WHBPUAD was obtained after solvent was evaporated under vacuum and deionized water was added to the reaction mixture with vigorous stirring (750–1200 rpm). The final solid content was 40 wt%.

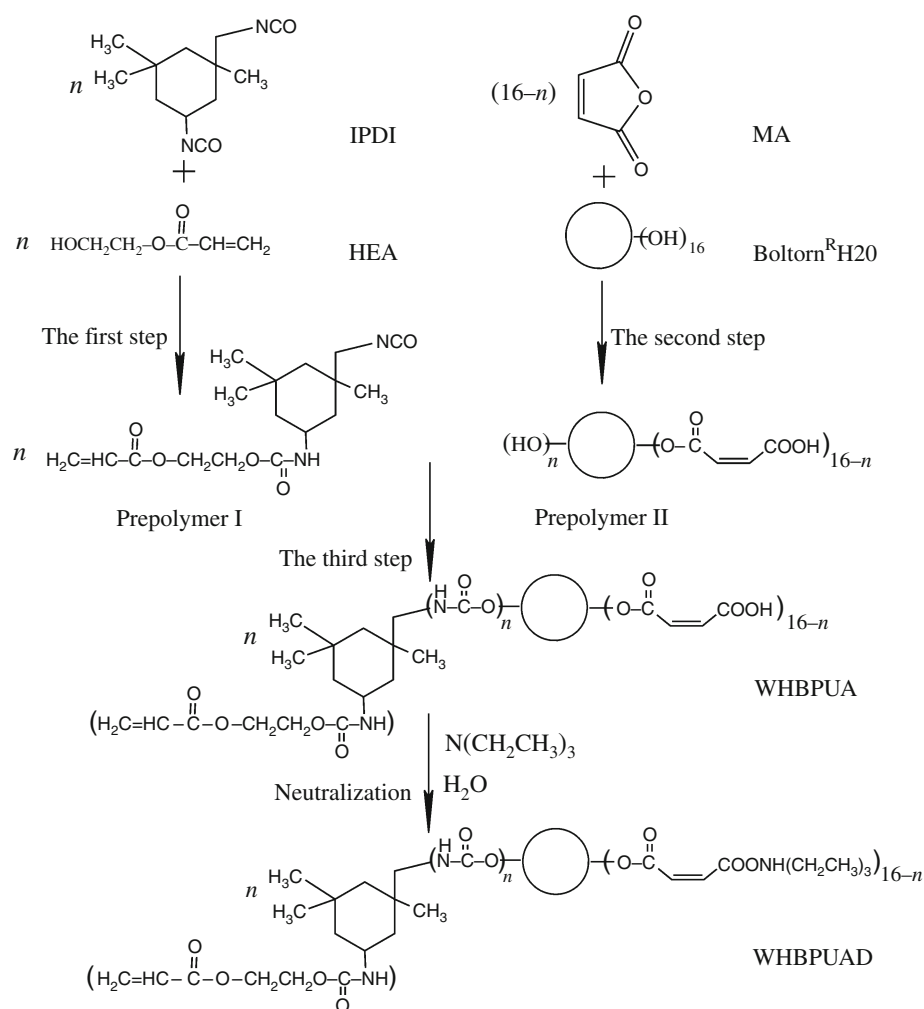Five types of WHBPUADs were synthesized and named as WHBPUAD 4-12, WHBPUAD 6-10,

Fig. 2: Reaction scheme for the synthesis of WHBPUAD

WHBPUAD 8-8, WHBPUAD 10-6, and WHBPUAD 12-4, respectively. The sample designations, compositions, end group types, initial acrylate double bond concentrations ($[M_0]$), and the viscosities of WHBPUADs are listed in Table 1.

Preparation of WHBPUAD films

The WHBPUADs were mixed with 2 wt% of Darocur 1173, and the films were prepared by a doctor blade technique on cleaned glass substrates at a typical thickness of 60 μm. The samples were dried at 50°C under vacuum, and then the UV-cured WHBPUAD films were obtained by exposing the sample under the UV radiation of a medium pressure mercury lamp (365 nm, 2 kW, 80 W cm^{-2}) which was made by Shenzhen Nengjia Automation Equipment Co., China. The maximum UV dose received by the irradiated sample was measured by radiometry to be on the order of 350 mJ cm^{-2} per 10 s.

Characterization

FTIR were recorded on a VECTOR 70 FTIR Spectrometer (Bruker, Germany) by scanning 32 times with a resolution of 4 cm^{-1}, within a spectral range of 400–4000 cm^{-1}. Samples for FTIR analysis were prepared by drying dispersions directly on KBr pellet. The nuclear magnetic resonance (^{1}H NMR) measurement was performed with an AVANCE 400 NMR Spectrometer (Bruker, Germany) at 25°C, CDCl$_3$ and TMS were used as solvent and internal standard substance, respectively.

The pendulum hardness of films was measured with a QBY pendulum damping tester (Tianjin Materials Laboratory Equipment Co, China) according to GB/T1730-1993 standards of China. The values, expressed in the time ratio with sample to glass, typically range from 0.07 for soft elastomeric materials up to 0.9 for very hard and glassy polymers. The flexibility of films was determined with YZQ-II cylindrical mandrel bend tester (Shanghai Pushen Chemical Industry Machinery

Table 1: Sample designation and composition of WHBPUADs

Samples	Molar ratio of raw material				Number of end group		$[M_0]$ (mmol g^{-1})	Viscosity (Pa s)
	IPDI	HEA	Boltorn®H20	MA	−C=C	−COOH		
WHBPUAD 4-12	4	4	1	12	4	12	0.94	0.7
WHBPUAD 6-10	6	6	1	10	6	10	1.26	0.9
WHBPUAD 8-8	8	8	1	8	8	8	1.53	3.9
WHBPUAD 10-6	10	10	1	6	10	6	1.75	9.6
WHBPUAD 12-4	12	12	1	4	12	4	1.94	16.9
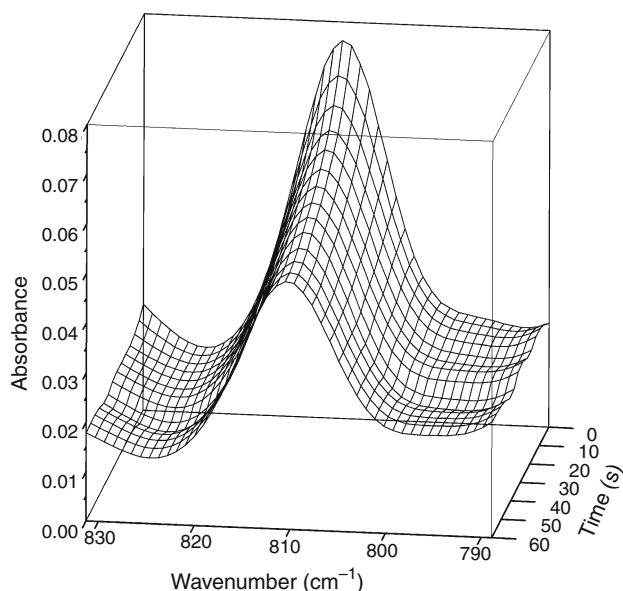
Fig. 3: Time dependence on UV exposure of the FTIR band at 810 cm^{-1} of the acrylate double bond of WHBPUAD

Fig. 4: FTIR spectra of prepolymer I (a), prepolymer II before (b) and after (c) synthesis and WHBPUAD (d)

Co., China) in accordance with GB 6742-86 standard. Impact resistance was performed on a CJQ-II paint film impact tester (Shanghai Pushen Chemical Industry Machinery Co., China), and adhesion was tested according to GB 1720-79(89) standard. Thermogravimetric analysis (TGA) was carried out with a TGA-60 thermoanalyzer (Schimadu Co., Japan). Approximately 5 mg of each sample was used at a heating rate of 20°C min^{-1} under N$_2$ from 30 to 650°C.

Study of the kinetics of photopolymerization

FTIR spectroscopy is applied to study the kinetics of photopolymerization reactions by recording the spectrum for every 10 s. Figure 3 shows a typical tridimensional representation of the variation of the FTIR spectrum in the 810 cm^{-1} region under UV exposure.

The kinetic conversion profiles are calculated from the decay of the absorption bands of the double bond group (CH=CH$_2$) twisting vibration at 810 cm^{-1}, and the characteristic absorption peak of carbonyl group (C=O) stretching mode at 1720 cm^{-1} is used as the internal standard peak by integration of the peak

areas.[14] Hence, the double bond conversion (τ) after a given exposure time (t) of CH=CH$_2$ can be readily obtained from the ratio of the FTIR absorbance areas before (A_0) and after UV irradiation (A_t) by equation 1.

$$\tau(\%) = \frac{(A_{810}/A_{1720})_0 - (A_{810}/A_{1720})_t}{(A_{810}/A_{1720})_0} \times 100 \qquad (1)$$

Results and discussion

FTIR of WHBPUAD

FTIR spectra of the prepolymers and WHBPUAD are shown in Fig. 4, traces a–d. A typical FTIR spectrum for prepolymer I shows the NCO group at 2267 cm^{-1}, carbonyl stretching band at 1730 cm^{-1}, N–H bending vibration at 1538 cm^{-1}, and the N–H stretching vibration at 3342 cm^{-1} from trace a in Fig. 4. The peaks at 1637, 1409, and 810 cm^{-1} associated with double bond indicate the existence of an acrylate group. The two peaks of 2956 and 2891 cm^{-1} are attributed to C–H stretching vibration of alkane. The FTIR spectra of the prepolymer II recorded before and after the synthesis

process are shown in traces b and c, respectively. The two peaks at 1849 and 1780 cm^{-1} due to the characteristic peaks of anhydride are prominent in trace b, but disappeared in trace c, indicating the anhydride groups of MA have totally taken part in the reaction. Furthermore, the decrease of peak intensity of terminal hydroxyl group in HBP at 3455 cm^{-1} illustrates that part of those hydroxyl groups have been involved in the half etherification reaction with MA. Finally, the disappearance of the peak at 2267 cm^{-1} due to NCO group in trace d indicates the reaction between prepolymer I and prepolymer II is completed.

^{1}H NMR spectrum of WHBPUAD

The ^{1}H NMR spectrum of the WHBPUAD is measured, and Fig. 5 shows a typical ^{1}H NMR spectrum. The peaks at δ = 6.5 ppm (a) and 6.15 ppm (b) are assigned to protons of double bonds in MA unit.[15] Meanwhile, the peaks at δ = 6.28, 6.15 and 5.88 ppm (a, b, and c) confirm the existence of acrylate groups in WHBPUAD molecular structure.[16] The single peaks at δ = 3.71 ppm (f) and 1.34 ppm (i) are attributed to the methylene groups adjacent to the hydroxyl end groups and methyl protons in the structure of HBP, respectively.[17] In addition, the peaks at δ = 1.86 (h), 1.18 (j), 1.07 (k), and 0.94 ppm (l) corresponding to the o-, p-, and methyl protons are relative to the hexatomic ring of IPDI, respectively. Therefore, the above results obtained using ^{1}H NMR confirm the formation of WHBPUAD, which is in accordance with the results of FTIR.

Photopolymerization kinetics

UV radiation curing has become a well-accepted technology, which can rapidly transfer liquid multifunctional monomers and oligomers into solid polymer coatings simply by exposure to UV radiation in the presence of a photoinitiator. Besides final degree of double bond conversion (τ^{f}), the maximum photopolymerization rate (R_{P}^{max}) is one of the important parameters for the efficiency of the process.

The double bond conversion (τ) as a function of polymerization time for WHBPUADs is shown in Fig. 6. From the conversion curves, the photopolymerization rates (R_{p}) are calculated according to equation 2.

$$R_{p} = [M_0] \times \frac{d\tau}{dt}, \qquad (2)$$

where $[M_0]$ is the initial acrylate double bond concentration.[14] The results are shown in Fig. 7.

As shown in Fig. 6, five types of WHBPUADs τ all increase with the increase of irradiation time, and follow the order of WHBPUAD 8-8 > WHBPUAD 12-4 > WHBPUAD 10-6 > WHBPUAD 4-12 > WHBPUAD 6-10 within first 200 s. After then, except for WHBPUAD 6-10, the reaction rates slow down. Because of vitrification, crosslinking is restricted and full conversion is not achieved. A certain amount of unreacted acrylate double bonds remained in the crosslinked polymer, which may ultimately affect the long-term properties of the UV-cured material.[18] The τ^{f} of WHBPUAD 8-8 reached a maximum value
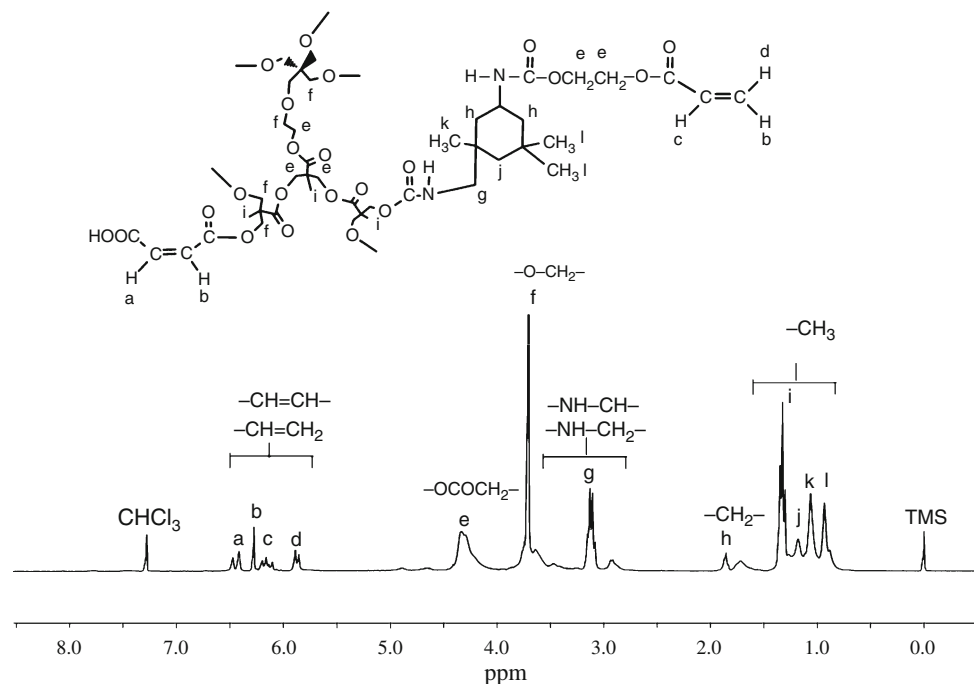
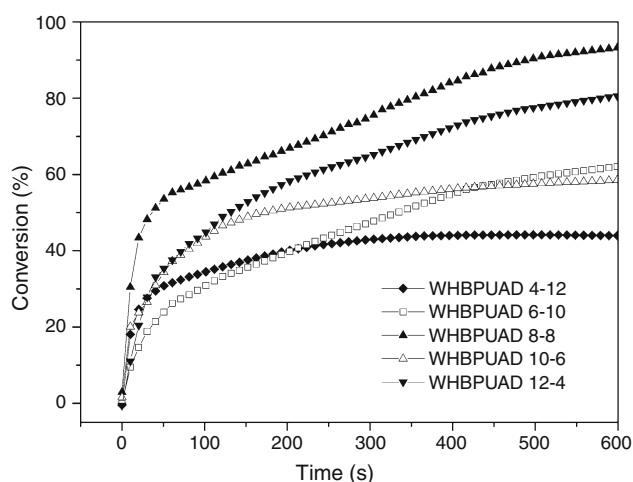**Fig. 5:** ^{1}H NMR spectrum of WHBPUAD

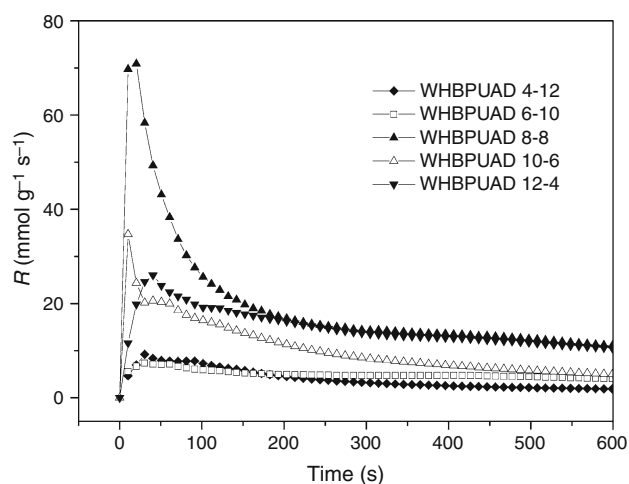**Fig. 6: Conversion of double bond of WHBPUADs**

Fig. 7: Photopolymerization rate of WHBPUADs

of 93%, compared to 81, 62, 58, and 49% of WHBPUAD 12-4, WHBPUAD 6-10, WHBPUAD 10-6, and WHBPUAD 4-12, respectively.

In Figs. 6 and 7, some typical features of the curing process are represented, such as autoacceleration and autodeceleration, which are in agreement with theoretical predictions.[14,19] The photopolymerization rate strongly depends on the mobility of the reactive chain ends, whereas the termination reaction is affected by the reduced mobility of the radical sites bound to the developing network.[20] At the low conversion, this leads to autoacceleration. In our study, as shown in Fig. 7, the photopolymerization rates of all five types increase sharply at the beginning, in the relatively low conversion, below about 30%, and the autoacceleration occurs until it reaches to the R_P^{max}. After the R_P^{max}, the photopolymerization rate decreases sharply, which is related the phenomena of autodeceleration. The R_P^{max} order of five types of WHBPUADs is as follows:

WHBPUAD 8-8 > WHBPUAD 10-6 > WHBPUAD 12-4 > WHBPUAD 4-12 > WHBPUAD 6-10.

The results can be explained with the double bond concentration and the viscosity of the UV-curable system.[21,22] In general, the higher concentration of double bonds of the acrylic end group located at the outer layer of the sphere-like structure may lead to higher R_p and τ. As a result, higher concentration of double bonds can obtain the higher R_p after irradiation for about 3 min as clearly seen in Fig. 6, and WHBPUAD 4-12 and WHBPUAD 6-10 with lower $[M_0]$ give lower R_p and τ in contrast to other WHBPUADs. In addition, the sequence of R_p and τ may be affected obviously by the viscosity of the UV-curable system. In the same radiation condition, the lower the viscosity of the UV-curable system, the more mobile and accessible are the reactive groups with unreacted acrylate double bonds, leading to higher R_p. For this reason, the R_p or τ of WHBPUAD 4-12 with lowest viscosity is higher than the R_p or τ of WHBPUAD 6-10 within first 200 s. After 200 s, the R_p or τ of WHBPUAD 4-12 is almost unchangeable since the $[M_0]$ is too low to keep the photopolymerization reaction. In the other side, with the polymerization proceeding, the viscosity of the irradiated system increases rapidly, the diffusion and mobility of both radicals and pendant double bonds are severely restricted in the vitrification network, leading to the fact that uncured double bonds trapped in the polymeric networks cannot keep the reaction. Accordingly, although WHBPUAD 12-4 has the highest $[M_0]$, the R_P^{max} and the τ^f are not the highest. Compared with the others, the WHBPUAD 8-8 has distinctly higher R_p and τ, and the R_P^{max}, the corresponding τ, as well as the time are 71 mmol g^{-1} s^{-1}, 43%, and 20 s, respectively.

## Film mechanical properties of WHBPUADs

The mechanical properties of WHBPUADs film are listed in Table 2. It shows that all of the coating formulations passed adhesion, impact, and flexibility tests at levels of 0 grade, 50 kg cm and 2 mm mandrel, respectively. The pendulum hardness follows the order of WHBPUAD 12-4 > WHBPUAD 10-6 > WHBPUAD 8-8 > WHBPUAD 6-10 > WHBPUAD 4-12, which are improved with the double bond concentration due to the crosslinking density after the UV irradiation. WHBPUAD 12-4 has the best mechanical properties with the maximum pendulum harnesses of 0.70%.

TGA of cured films of WHBPUADs

The TGA curves of UV-cured WHBPUADs films and their corresponding derivative weight loss curves (DTG) are shown in Figs. 8 and 9, respectively. As seen in the figures, all samples have a similar process of thermal decomposition, which appears as three

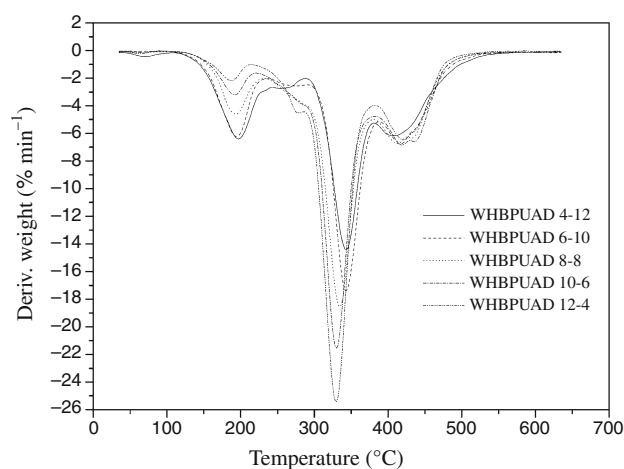**Table 2: Mechanical properties of the UV-cured film of WHBPUADs**

Samples	Adhesion (grade)	Impact strength (kg cm)	Flexibility (mm)	Pendulum hardness (%)
WHBPUAD 4-12	0	50	1	0.08
WHBPUAD 6-10	0	50	1	0.17
WHBPUAD 8-8	0	50	1	0.55
WHBPUAD 10-6	0	50	1	0.62
WHBPUAD 12-4	0	50	1	0.70
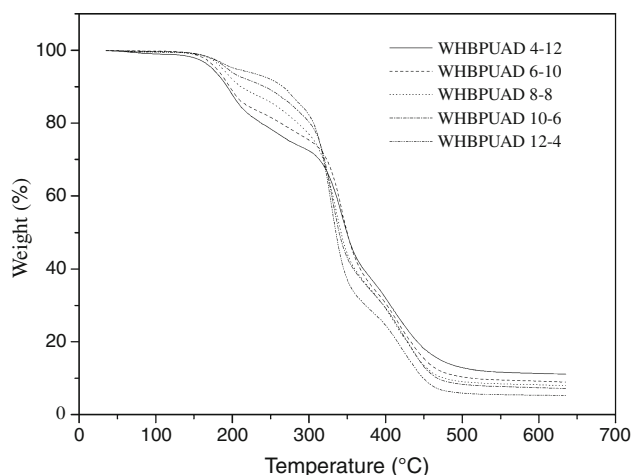
Fig. 8: TGA curves of the cured films of WHBPUADs

Fig. 9: DTG curves of the cured films of WHBPUADs

obvious weight loss regions with peak maxima around 195, 335, and 415°C, respectively. Region I may be assigned to the decomposition of the ester of carboxylic acids terminal (H20-MA) and the urethane of the hard segment (IPDI-HEA). Region II which has lost the most weight may correspond to the decomposition of the soft segment.[23,24] Region III may be related to the core degradation of Boltorn®H20.

As is well known, the degradation in the early stage plays an important role among the overall thermal stability of a polymer. In order to validate the decomposition of region I, the weight percentage of carboxylic acids terminal (H20-MA) and hard segment (IPDI-HEA) group are calculated and compared with the measured values. The initial decomposition temperature corresponding to region I, region II, region III, as well as calculated and measured weight loss at region I are summarized in Table 3. The experimental results show that the values of calculated and measured are in agreement suggesting that carboxylic acids terminal (H20-MA) and hard segment (IPDI-HEA) groups decompose first. In addition, below about 330°C, the thermal decomposition rate sequence is WHBPUAD 4-12 > WHBPUAD 6-10 > WHBPUAD 8-8 > WHBPUAD 10-6 > WHBPUAD 12-4.

The heat resistance of the cured films is improved with the increase in double bond concentration ($[M_0]$). For instance, with the increase of $[M_0]$ from 0.94 mmol g^{-1} (WHBPUAD 4-12) to 1.94 mmol g^{-1} (WHBPUAD 12-4), the initial decomposition temperature (T_i) which is represented by 5% weight loss temperature rises to 202.7°C from 173.9°C. The improvements of heat resistance are attributed to the increasing of crosslinking density of the cured films. Samples with higher double bond concentration are sure to obtain films with higher crosslinking density after being cured by UV, which possess better heat resistance. These results are coincident with those reported by Asif et al.[25] Moreover, after region I (over 330°C), the thermal decomposition rate order is opposite, which is WHBPUAD 4-12 < WHBPUAD 6-10 < WHBPUAD 8-8 < WHBPUAD 10-6 < WHBPUAD 12-4, with the final weight residues at 650°C of the cured films being 11.1, 8.9, 7.9, 7.1, and 5.2%, respectively.

Conclusions

In the present work, five types of UV-curable WHBPUADs with different double bond concentration were successfully prepared and their structure was confirmed by FTIR and ^{1}H NMR. The investigation of the photopolymerization kinetics indicated that the photopolymerization rate and the double bond conversion were co-affected by the double bond concentration and the viscosity. The higher double bond concentration or lower viscosity could result in higher τ and R_p. According to this, WHBPUAD 8-8 had the highest photopolymerization rate (71 mmol g^{-1} s^{-1}) and the maximum final double bond conversion (93%).

Table 3: T_i, calculated and observed weight loss for decomposition of WHBPUADs

Samples	T_i (°C)			Calculated weight loss (%)			Observed weight loss at region I (%)
	Region I	Region II	Region III	MA	HEA	Total	
WHBPUAD 4-12	173.9	322.8	356.8	27.5	10.9	38.4	37.5
WHBPUAD 6-10	179.1	324.8	357.1	20.6	14.7	35.3	33.8
WHBPUAD 8-8	186.9	315.6	347.4	15.0	17.8	32.8	31.0
WHBPUAD 10-6	193.1	313.3	342.3	10.3	20.3	30.6	26.7
WHBPUAD 12-4	202.7	312.6	342.6	6.3	22.5	28.8	25.9

UV-cured films were found to exhibit superior mechanical properties, and the pendulum hardnesses were improved with the increase in double bond concentration. The UV-cured film of WHBPUAD 12-4 had the highest pendulum hardnesses at the value of 0.70%. All the WHBPUAD samples showed three obvious decomposition regions represented by the carboxylic acids terminal (H20-MA) and hard segment (IPDI-HEA), the soft segment and the core degradation of the HBP, respectively.

References

1. Schwalm, R, Haubling, L, Reich, W, Beck, E, Enenkel, P, Menzel, K, "Tuning the Mechanical Properties of UV Coatings Towards Hard and Flexible Systems." *Prog. Org. Coat.*, **32** (1–4) 191–196 (1997)
2. Decker, C, Lorinczova, I, "UV-Radiation Curing of Waterborne Acrylate Coatings." *J. Coat. Technol. Res.*, **1** (4) 247–256 (2004)
3. Kim, BK, "Aqueous Polyurethane Dispersions." *Colloid Polym. Sci.*, **274** 599–611 (1996)
4. Liu, D, Zeng, SM, Yao, C, Chen, AF, Chen, ZH, Xu, ZS, "Synthesis and Properties of Hyperbranched Aqueous Poly(urethane-urea) via A(2) + bB(2) Approach." *Polym. Bull.*, **63** (2) 213–224 (2009)
5. Overbeek, A, "Polymer Heterogeneity in Waterborne Coatings." *J. Coat. Technol. Res.*, **7** (1) 1–21 (2010)
6. Yang, ZL, Wicks, DA, Hoyle, CE, Pu, HT, Yuan, JJ, Wan, DC, Liu, YS, "Newly UV-Curable Polyurethane Coatings Prepared by Multifunctional Thiol- and Ene-Terminated Polyurethane Aqueous Dispersions Mixtures: Preparation and Characterization." *Polymer*, **50** (7) 1717–1722 (2009)
7. Asif, A, Shi, WF, Shen, XF, Nie, KM, "Physical and Thermal Properties of UV Curable Waterborne Polyurethane Dispersions Incorporating Hyperbranched Aliphatic Polyester of Varying Generation Number." *Polymer*, **46** (24) 11066–11078 (2005)
8. Tryson, GR, Shultz, AR, "A Calorimetric Study of Acrylate Photopolymerization." *J. Polym. Sci. Polym. Phys. Ed.*, **17** (12) 2059–2075 (1979)
9. Pappas, SP, *Radiation Curing: Science and Technology*. Plenum Press, New York (1992)
10. Scherzer, T, Decker, U, "Real-time FTIR-ATR Spectroscopy to Study the Kinetics of Ultrafast Photopolymerization Reactions Induced by Monochromatic UV Light." *Vib. Spectrosc.*, **19** (2) 385–398 (1999)
11. Scherzer, T, Langguth, H, "The Effect of Temperature on the Induction Period in the Photoinitiated Polymerization of Tripropylene Glycol Diacrylate." *Nucl. Instrum. Methods Phys. Res. Sect. B*, **185** 276–282 (2001)
12. Lin, JN, Zeng, XR, Hou, YJ, Shi, HJ, "Synthesis and Characterization of UV-Curable Hyperbranched Urethane Acrylate." *Polym. Plast. Technol. Eng.*, **47** (3) 237–241 (2008)
13. Gao, Q, Li, H, Zeng, X, "Preparation and Characterization of UV-Curable Hyperbranched Polyurethane Acrylate." *J. Coat. Technol. Res.*, **8** (1) 61–66 (2011)
14. Decker, C, "Photoinitiated Crosslinking Polymerisation." *Prog. Polym. Sci.*, **21** (4) 593–650 (1996)
15. Hong, C-Y, You, Y-Z, Liu, J, Pan, C-Y, "Dendrimer-Star Polymer and Block Copolymer Prepared by Reversible Addition-Fragmentation Chain Transfer (RAFT) Polymerization with Dendritic Chain Transfer Agent." *J. Polym. Sci. A Polym. Chem.*, **43** (24) 6379–6393 (2005)
16. Xu, G, Shi, WF, "Synthesis and Characterization of Hyperbranched Polyurethane Acrylates Used as UV Curable Oligomers for Coatings." *Prog. Org. Coat.*, **52** (2) 110–117 (2005)
17. Zhang, J, Hu, CP, "Synthesis, Characterization and Mechanical Properties of Polyester-Based Aliphatic Polyurethane Elastomers Containing Hyperbranched Polyester Segments." *Eur. Polym. J.*, **44** (11) 3708–3714 (2008)
18. Decker, C, "The Use of UV Irradiation in Polymerization." *Polym. Int.*, **45** (2) 133–141 (1998)
19. Scherzer, T, Decker, U, "The Effect of Temperature on the Kinetics of Diacrylate Photopolymerizations Studied by Real-Time FTIR Spectroscopy." *Polymer*, **41** (21) 7681–7690 (2000)
20. Fouassier, J-P, *Radiation Curing in Polymer Science and Technology*. Elsevier, London (1993)
21. Sun, F, Shi, J, Du, HG, Nie, J, "Synthesis and Characterization of Hyperbranched Photosensitive Polysiloxane Urethane Acrylate." *Prog. Org. Coat.*, **66** (4) 412–419 (2009)
22. Decker, C, Masson, F, Schwalm, R, "How to Speed Up the UV Curing of Water-Based Acrylic Coatings." *J. Coat. Technol. Res.*, **1** (2) 127–136 (2004)
23. Cacute, ZSP, Zavargo, Z, Flyn, JH, Macknight, WJ, "Thermal Degradation of Segmented Polyurethanes." *J. Appl. Polym. Sci.*, **51** (6) 1087–1095 (1994)
24. Yeganeh, H, Shamekhi, MA, "Poly(urethane-imide-imide), a New Generation of Thermoplastic Polyurethane Elastomers with Enhanced Thermal Stability." *Polymer*, **45** (2) 359–365 (2004)
25. Asif, A, Hu, LH, Shi, WF, "Synthesis, Rheological, and Thermal Properties of Waterborne Hyperbranched Polyurethane Acrylate Dispersions for UV Curable Coatings." *Colloid Polym. Sci.*, **287** (9) 1041–1049 (2009)